ТЕСЛИНИ ИНОВАЦИОНИ ДАНИ
TESLA INNOVATION DAYS
Belgrade, Serbia, April 7 - 8, 2025

DOI: 10.5937/TID25016R

APPLICATION OF THE NONLINEAR KERNEL PRINCIPAL COMPONENT ANALYSIS IN DETECTING DISK-TO-DISK FAULTS ALONG A TRANSFORMER WINDING

Ebrahim Rahimpour[1*], Mohammed Bilal Ghorbal [2], Hassan Reza Mirzaei[2]

[1]Technical University of Applied Sciences Würzburg-Schweinfurt, Schweinfurt, Germany
[2]Department of Electrical Engineering, University of Zanjan, Zanjan, Iran

Abstract

Rapid and accurate identification of short-circuit (SC) faults in transformer windings is essential to ensure power system reliability and reduce the need for extensive, costly laboratory testing. Since SC faults often originate from transient overvoltages in the grid, reliable diagnostic techniques are required to determine both their location and severity. Among these techniques, the Frequency Response Analysis (FRA) method is widely recognized for its effectiveness in detecting electrical faults in transformer windings under controlled High-Voltage (HV) laboratory conditions. This paper investigates an HV, single, specially fabricated disc winding and measures its Frequency Responses (FRs) under both healthy and disc-to-disc SC conditions using the FRA method. A detailed electrical model of the winding is then developed using analytical expressions. Various SC scenarios are systematically introduced into the model, and the corresponding FRs are simulated. The simulated results are validated against measured FRs, confirming the accuracy of the modeling approach. To further enhance fault characterization, Kernel Principal Component Analysis (KPCA) is applied to the simulated FRs to extract salient features and cluster them in a low-dimensional space based on fault location. The findings demonstrate the potential of combining FRA-based measurements, detailed modelling, and nonlinear feature extraction as a foundational step toward reliable SC fault detection in practical transformer windings.

Keywords: Disc-to-Disc Fault, short circuit detection, low voltage impulse method, feature extraction.

1 Introduction

Transient overvoltages in power networks can impose severe electrical stresses on transformer winding insulation. In disc-type windings, these stresses are distributed unevenly across the insulation spacers between adjacent discs. When the electric stress across a disc-to-disc insulation exceeds its dielectric strength, breakdown occurs, resulting in a Short-Circuit (SC) or Disc-to-Disc Fault (DDF). According to [1], approximately 30% of transformer failures are associated with winding-related faults. Therefore, detecting and accurately diagnosing such faults, followed by timely maintenance, are essential to prevent high SC currents from propagating through the winding and triggering further damage. This, in turn, extends transformer service life, enhances power system reliability, and reduces the likelihood of widespread outages.

A variety of monitoring techniques are available for assessing transformer health, including dissolved gas-in-oil analysis and thermal monitoring based on load current and temperature [2]. Moreover, Frequency Response Analysis (FRA) is among the most widely used techniques for identifying both electrical and mechanical defects in transformer windings [3]. Using FRA, numerous studies have focused on distinguishing DDFs from mechanical deformation faults, including axial displacement, radial deformation, and disc-spacing variations [3, 4]. In [4], a comparison index, referred to as the windowed calculation index, was introduced to compute numerical indicators from each Frequency Response (FR). These indicators were then processed using Fisher Discriminant Analysis (FDA), a linear dimensionality reduction method, to extract features for fault classification. Additionally, the authors in [3] employed vector fitting to estimate the polynomial and real coefficients of rational functions representing the FRs of the test winding. These coefficients were subsequently used as inputs to a probabilistic neural network to classify multiple fault types. Further, in [5], statistical control charts were utilized to interpret FRA results and improve discrimination between electrical and mechanical faults. Mathematical tools such as cross-correlation and standard deviation have also been explored to compute essential features for training multilayer perceptrons to identify winding fault types [6].

Other studies have investigated Artificial Neural Network (ANN)-based approaches to determine the location and severity of DDFs in various transformer windings [7]. In [8], only measured FRs obtained from healthy and faulty windings were directly fed into a Support Vector Regression (SVR)

model to estimate the fault location. Deep learning techniques have also been explored; for example, Convolutional Neural Networks (CNNs) have been applied to classify DDFs in distribution transformer windings using image-based representations of FRs [9]. Moreover, statistical indices remain a powerful tool for quantifying FR similarity and determining DDF locations [10].

Despite these advancements, many existing techniques rely on linear feature extraction methods or predefined statistical indicators, which may not fully capture the nonlinear behavior of FR variations under electrical fault conditions. To address this limitation, the present study investigates the effectiveness of Kernel Principal Component Analysis (KPCA), a nonlinear dimensionality reduction technique, in extracting and clustering features from FRs of a single High-Voltage (HV) disc winding under intact and SC conditions. The capability of KPCA to reveal distinct low-dimensional clusters corresponding to different fault locations is also evaluated.

The remainder of this paper is organized as follows. Section 2 describes the modeling methodology for the test winding. Section 3 validates the developed model by comparing simulated and experimentally measured FRs. Section 4 describes the KPCA algorithm. Section 5 illustrates the detection of DDFs in the test winding. Finally, Section 6 summarizes the key findings and contributions of this study.

2 Modeling of the HV winding

The detailed model, including all R-L-C-M elements, is widely recognized as an appropriate representation for studying electrical faults in disc-type transformer windings over a frequency range up to 1 MHz [3]. The test winding used in this study is illustrated in Fig. 1(a), and its geometric dimensions are provided in Fig. 1(b). The winding consists of 60 discs, each comprising 9 turns. In the modeling process, every two consecutive discs are grouped into a single unit, resulting in 30 units in the detailed model shown in Fig. 2.

Each model unit is represented by a set of R-L-C-M elements. The series resistance, R_{Si}, accounts for conductor (copper) losses, while R_{Pi} and R_{ei} represent series and parallel insulation losses, respectively. The self-inductance of the i^{th} unit is denoted by L_{Si}, and the mutual inductance between the i^{th} and j^{th} units is represented by $M_{i,j}$. The series capacitance is modeled by K_i, whereas the shunt capacitance to ground is represented by C_{ei}. Since the test winding does not include a magnetic core, a shielded copper cylinder is placed inside the winding to emulate the elements R_{ei} and C_{ei}, which correspond to the electric coupling between the winding and an equivalent core. All R-L-C-M components are calculated using a set of analytical expressions described in [11].

The FRA technique can be performed either in the time domain using a Low Voltage Impulse (LVI) or in the frequency domain using the Swept Frequency Response Analysis (SFRA) method [12, 13]. In the winding modelling, the SFRA approach is

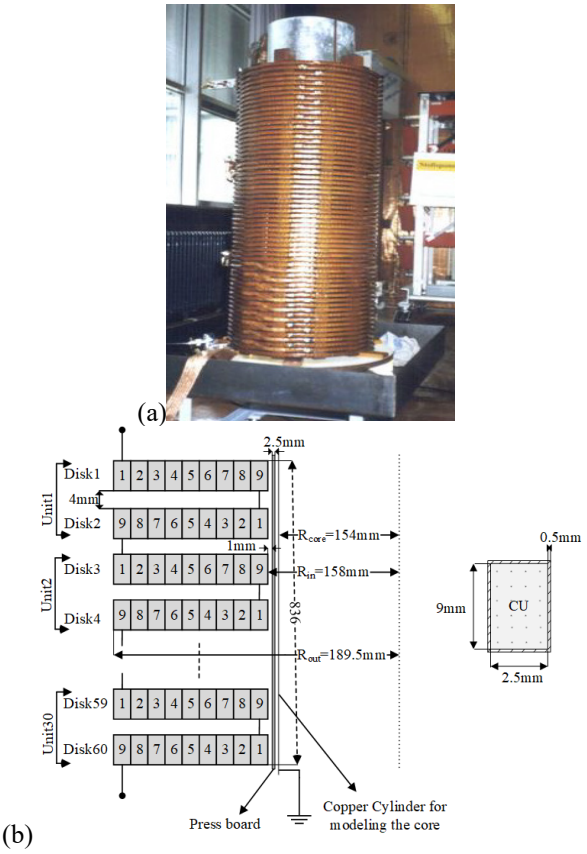


Figure 1. The configuration of the HV test winding (a), and its geometric dimensions (b)

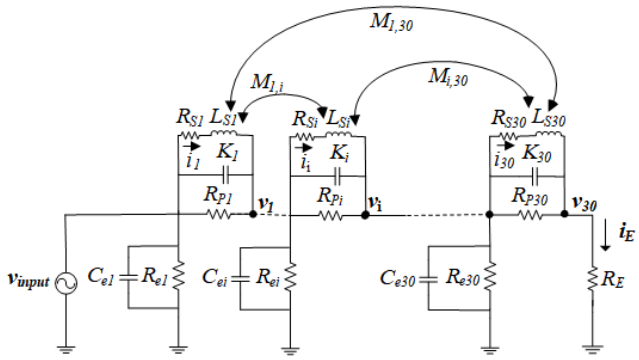


Figure 2. The detailed R-L-C-M model of the test winding comprises 30 units. R_E: grounding resistance.

employed to compute the FRs of the winding model shown in Fig. 2 under healthy conditions. In this method, a sinusoidal excitation voltage v_{input} with continuously varying frequency is applied to the model, and the resulting output v_{30} is calculated. The corresponding earth current i_E, flowing through a 50 Ω grounding resistor R_E, is then determined. Both v_{30} and i_E are obtained by applying Kirchhoff's laws to the detailed R-L-C-M network of Fig. 2, leading to the matrix formulation expressed in (1):

$$[Y][U] = [A][I] + [B_1]$$
$$[Z][I] = [A^T][U] + [B_2] \quad (1)$$

where:

$$I = [i_1 \quad \dots \quad i_{30}]^T,\ U = [v_1 \quad \dots \quad v_{30}]^T$$

Moreover, the elements A, B_1, B_2, and Z are provided in detail in [12], and Y is computed as:

$$[Y] = \begin{bmatrix} Y_{e1}+Y_{P1} & -Y_{P1} & 0 & \dots & \dots & 0 \\ -Y_{P1} & Y_{e2}+Y_{P1}+Y_{P2} & -Y_{P2} & 0 & \dots & 0 \\ \dots & \dots & \dots & \dots & \dots & \dots \\ 0 & \dots & \dots & -Y_{P28} & Y_{e29}+Y_{P29}+Y_{P30} & -Y_{P29} \\ 0 & \dots & \dots & \dots & -Y_{P29} & Y_{e30}+Y_{P30} \end{bmatrix}$$

where $Y_{Pi} = (j2\pi f K_{Pi} + 1/R_{Pi})$, $Y_{ei} = (j2\pi f C_{ei} + 1/R_{ei})$, and f denotes the applied frequency.

Using the applied voltage, v_{input}, and the calculated current, i_E, in the frequency domain, the required FR can be calculated as follows [13]:

$$FR(f) = \left| \frac{i_E(f)}{v_{input}(f)} \right| \tag{2}$$

2.1 Simulation of the Disc-to-Disc faults

To simulate a DDF at the i^{th} unit, a fault resistance, R_{SCi}, is inserted between its terminals as shown in Fig. 3. This resistance modifies the admittance matrix through the term, $Y_{SCi} = 1/R_{SCi,}$ which is added to the appropriate elements of the Y matrix as follows:

$$Y(i-1,i-1) = (Y_{P(i-1)} + Y_{Pi} + Y_{ei} + Y_{SCi})$$
$$Y(i-1,i) = Y(i,i-1) = -(Y_{Pi} + Y_{SCi})$$
$$Y(i,i) = (Y_{Pi} + Y_{P(i+1)} + Y_{e(i+1)} + Y_{SCi})$$

After applying v_{input} to the updated model (Fig. 3), the resulting i_E is computed and used to obtain the associated FR using Eq. (2). Applying a DDF with a specific R_{SCi} to each of the 30 units yields 30 distinct FRs. Furthermore, changing the value of R_{SCi} can alter the severity of DDF at the faulty unit. Therefore, applying n DDF with different severity levels to all units individually produces 30×n FRs, enabling systematic analysis of fault magnitude.

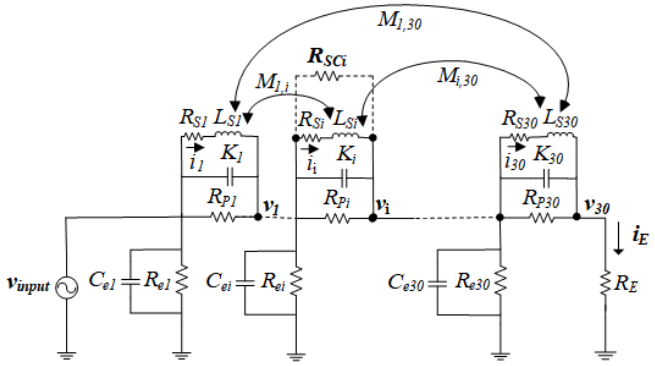


Figure 3. Applying the DDF to the detailed model in the i^{th} unit by linking its terminals to the fault resistance, R_{SCi}.

3 Validation of the modelling

To verify the obtained detailed model, its simulated FR under both healthy and SC conditions should be compared with the measured ones. Therefore, the LVI method is used to obtain the measured FRs of the winding. In this method, a low-voltage generator is used to apply an impulse voltage with front and tail times of 1.1 and 38.6 µs, respectively. Then, the output current is measured using a Rogowski Coil that records the current signal at 126 kHz to several MHz [12]. The input voltage and output current signals are then filtered and transformed to the frequency domain using the Fast Fourier Transform (FFT). Then, the measured FR can be calculated by dividing the current signal by the voltage signal. The FR of the winding is also measured after directly short-circuiting each consecutive pair of discs of the test winding. Therefore, in addition to the FR associated with the winding under healthy conditions, 30 measured FRs related to short-circuiting every two adjacent discs individually are also recorded.

To determine the accuracy of the winding model, the measured and simulated FRs obtained from the winding under healthy conditions are compared in Fig. 4. Furthermore, to further ensure the accuracy of the simulation, the measured and simulated FRs obtained after the occurrence of a DDF individually at units 12 and 15 with $R_{SCi} = 0\ \Omega$ are compared in Fig. 5(a) and 5(b). It can be demonstrated from Fig. 4 and Fig. 5 that the acceptable agreement between the measured and simulated FRs proves the accuracy of the modelling. Therefore, the validated model can be used to simulate other DDFs with different severities.

Unit 15 is located in the middle of the model; therefore and after attention to the measured and simulated FRs obtained after applying DDF to all winding units individually, it can be observed a kind of symmetry between the FRs of the upper (units 1 to 15) and lower (units 16 to 30) halves of the winding. For clarity, from Fig. 6, the symmetry between the measured FRs resulting from direct short-circuiting the units 10 and 15 of the upper half by the fault resistance $R_{SCi} = 0\ \Omega$, with that related to units 16 and 21 of the lower half, respectively. Therefore, this symmetry can complicate discrimination between the DDF that occurred on a unit of the upper half and its corresponding one in the lower half.

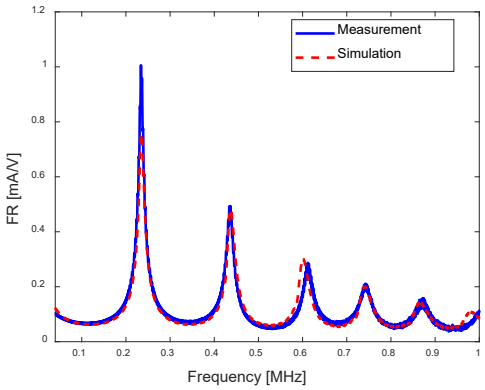


Figure 4. Comparison between simulated and measured FRs of the winding under intact condition.

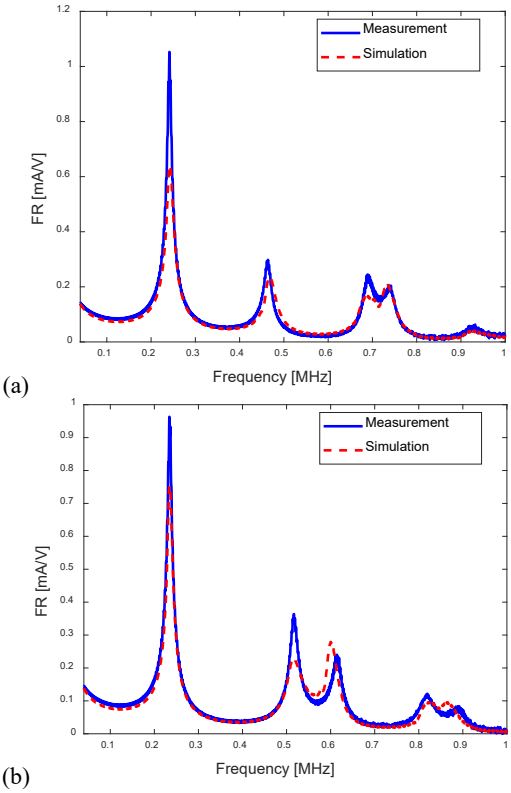


Figure 5. Comparison between simulated and measured FRs of the winding when occurrence SC with $R_{SCi} = 0\ \Omega$ at units 12 (a) and 15 (b).

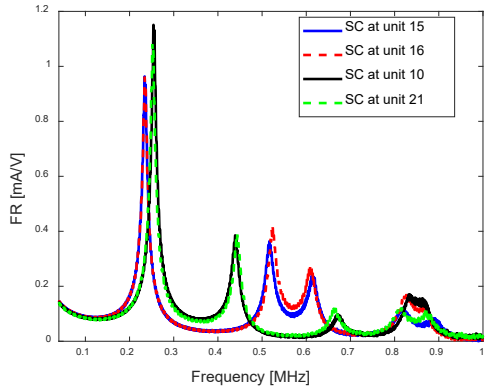


Figure 6. Symmetry in the measured frequency responses obtained from applying SC with $R_{SCi} = 0\ \Omega$ on units 15 and 16, and between units 10 and 21.

4 Kernel Principal Component Analysis (KPCA) method

Each FR of the winding related to healthy or DDF conditions is a nonlinear High-Dimensional (HD) data set containing D frequency samples; therefore, applying various DDFs with different severity levels to all winding units will produce N nonlinear FRs. Then, if these FRs are arranged in an HD matrix, called the Frequency Response Matrix (FRM), the dimensions of this matrix will be $N \times D$ as follows:

$$FRM = \begin{bmatrix} FR_1 \\ FR_2 \\ \dots \\ FR_{N-1} \\ FR_N \end{bmatrix} = \begin{bmatrix} FR_{1,1} & \dots & FR_{1,D} \\ FR_{2,1} & \dots & FR_{2,D} \\ \dots & \dots & \dots \\ FR_{N-1,1} & \dots & FR_{N-1,D} \\ FR_{N,1} & \dots & FR_{N,D} \end{bmatrix}_{N \times D}$$

To reduce the dimensionality of the FRM, an appropriate nonlinear dimension-reduction algorithm should be employed to extract key features and visualize them in a lower-dimensional space. Therefore, KPCA is a powerful nonlinear dimensionality reduction method that extends traditional PCA by first mapping the data to a high-dimensional space via a kernel function and then performing principal component analysis in that space [14]. Instead of explicitly computing the mapping function, this method uses the kernel trick to compute a Kernel Matrix (KM):

$$KM = \begin{bmatrix} KM_1 \\ KM_2 \\ \dots \\ KM_{N-1} \\ KM_N \end{bmatrix} = \begin{bmatrix} KM_{1,1} & \dots & KM_{1,N} \\ KM_{2,1} & \dots & KM_{2,N} \\ \dots & \dots & \dots \\ KM_{N-1,1} & \dots & KM_{N-1,N} \\ KM_{N,1} & \dots & KM_{N,N} \end{bmatrix}_{N \times N}$$

Each element of the KM is obtained using standard kernel functions, such as the Gaussian and polynomial kernels, which are described by expressions 3 and 4, respectively [14]:

$$KM_{i,j} = \exp\left(\frac{-\left\|FR_i - FR_j\right\|^2}{2\sigma^2}\right) \quad (3)$$

$$KM_{i,j} = (FR_i + FR_j + 1)^d \quad (4)$$

where $2\sigma^2$ is the width of the Gaussian kernel and d is a positive number determined by the trial-and-error method. In general, similar results should be obtained when selecting appropriate kernel parameters for expressions 3 and 4.

In the next step, the resulting KM must be centered, and the PCA algorithm must be used to extract the eigenvectors and eigenvalues of the calculated KM. By this method, each FR can be projected as a 2D feature point in a feature space through a weighted combination of kernel evaluations. This process not only reduces the dimensionality of the FRM but also preserves the geometric structure and nonlinear complexities of the FRs. For this reason, KPCA is highly effective and applicable to tasks such as error detection, pattern recognition, and classification [15].

By applying the PCA algorithm to the KM and calculating the related eigenvectors and eigenvalues, the high-dimensional FRM with dimensions of $N \times D$, including all FRs, will be transformed to a 2D matrix, including all related 2D Extracted Features (EFs) as follows:

$$EF == \begin{bmatrix} EF_{1,1} & EF_{1,2} \\ EF_{1,2} & EF_{2,2} \\ \dots & \dots \\ EF_{N-1,1} & EF_{N-1,2} \\ EF_{N,1} & EF_{N,2} \end{bmatrix}_{N\times 2}$$

More details on KPCA for calculating eigenvectors, eigenvalues, and 2D features are available in [14, 15].

5 Detecting Disc-to-Disc Faults

Validation of the winding model is a crucial prerequisite before introducing DDFs and analyzing their corresponding FRs. To this end, solid DDFs are first simulated by applying a fault resistance of R_{SCi} = 0 Ω sequentially to each unit of the model, and the resulting 30 FRs are computed and stored in a *FRM*. This procedure is then repeated for higher fault resistances of R_{SCi}=10, 30, 50, 70, and 100 Ω, which represent different fault severities, with the corresponding FRs appended to the *FRM*. As a result, in addition to the FR of the healthy winding, the *FRM* contains a total of 180 FRs corresponding to various DDF conditions. Moreover, a DDF with R_{SCi} = 37 Ω is applied to unit 13 as a new DDF to demonstrate the KPCA algorithm's ability to estimate the location and severity of any new fault along the winding. Then its FR is added to the *FRM*.

To show some simulated FRs of the model when exposing it to different DDFs, Figs. 7(a) and 7(b) present representative simulated FRs obtained when DDFs are applied to model units 1, 10, 15, 20, and 30 using fault resistances R_{SCi} = 0 and 50 Ω, respectively. As evident from these figures, increasing the fault resistance, corresponding to a reduction in fault severity, leads to a noticeable decrease in the magnitude of the FRs, while the resonance frequencies remain largely unchanged.

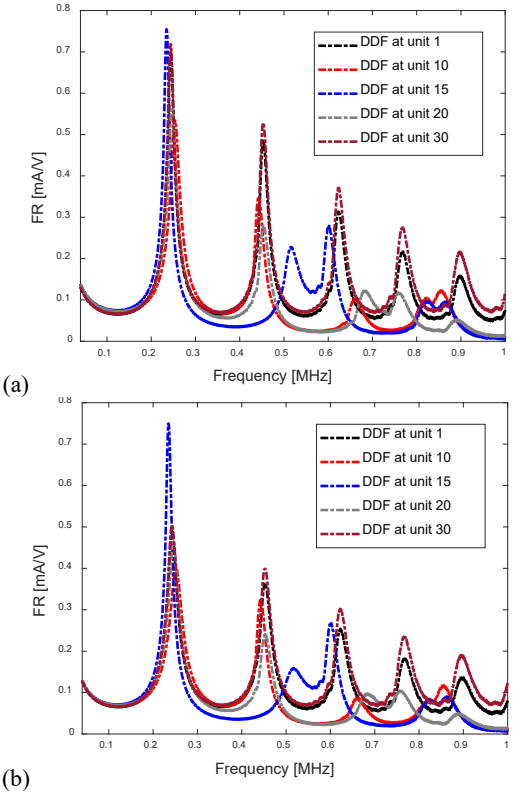


Figure 7. The simulated frequency responses of the winding when applying a DDF, with (a) R_{SCi} =0 Ω, and (b) R_{SCi} =50 Ω, to units 1, 10, 15, 20, and 30 individually

Applying the KPCA algorithm to the 182 FRs stored in the *FRM* will result in 182 *EFs* in the 2D space. Therefore, using the trial-and-error method, the KPCA with a polynomial kernel of degree 3 is applied to the *FRM*, and the resulting *EFs* are shown in Fig. 8(a). Furthermore, applying the Gaussian kernel with σ = 6 yields the *EFs* shown in Fig. 8(b). In these figures, the number of each unit is shown near its features. Moreover, it can be observed from Fig. 8(a) and 8(b) that the feature points associated with a unit are clustered. In addition, the symmetrical behaviour between the FRs related to the upper and lower units in the HD space is evident in the 2D space. For instance, the *EFs* for units 5 and 26 form two clusters with a very small distance. Furthermore, it is clear that increasing the fault resistance R_{SCi} shifts the related *EFs* towards the healthy conditions feature. Also, the *EF* obtained by applying the new DDF at unit 13 by R_{SCi} = 37 Ω is projected in the cluster associated with unit 13 and located between the *EFs* corresponding to DDFs with R_{SCi}= 30 and 50 Ω. Consequently, selecting the suitable parameters of the KPCA, including the degree of the polynomial and the variance of the Gaussian kernels, visualizes 2D feature points related to simulated FRs in separate clusters inside the feature space. Therefore, by comparing the distances between the feature points of the new DDFs that occur in the winding and the formed clusters in the 2D space, their locations and severities can be detected with acceptable accuracy.

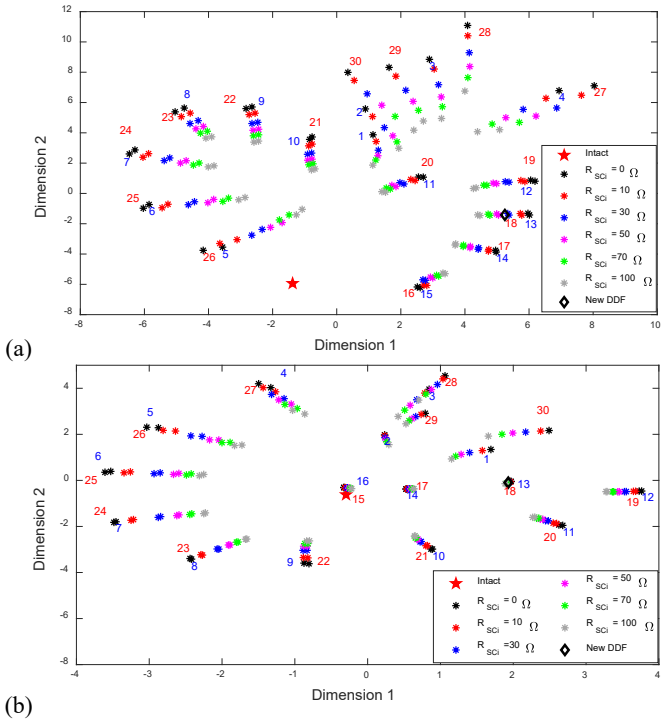


Figure 8. The extracted features obtained by applying the KPCA, with (a) polynomial, and (b) Gaussian kernels, to the FRs related to healthy and DDF conditions with R_{SCi} = 0, 10, 30, 50, 70, and 100 Ω, and FR associated with the new DDF.

6 Conclusion

This paper presented a comprehensive FRA-based framework for detecting and localizing disc-to-disc short-circuit faults in transformer windings using nonlinear feature extraction. A detailed R–L–C–M model of a specially fabricated HV disc winding was developed and validated through close agreement between simulated and experimentally measured frequency responses under both healthy and faulty conditions. The validated model enabled systematic simulation of disc-to-disc faults with varying locations and severities, providing a reliable dataset for advanced diagnostic analysis.

The KPCA algorithm was applied to the resulting high-dimensional FR data to extract salient nonlinear features and project them into a low-dimensional space. The results showed that KPCA effectively clusters FRs by fault location while preserving the progression of fault severity. Both polynomial and Gaussian kernels successfully revealed distinct feature groupings when appropriate kernel parameters were selected, confirming the suitability of KPCA for capturing the nonlinear behavior of FRA signatures associated with SC faults. Moreover, it was shown that the KPCA algorithm, by projecting the FRs of new DDFs into a 2D space, can reliably estimate their location and severity. These findings highlight the potential of combining detailed winding modeling, FRA measurements, and nonlinear dimensionality-reduction techniques as a powerful diagnostic tool for transformer winding condition assessment. Future work should focus on extending the presented methodology to more complex transformer configurations, including multi-winding and core-type transformers, and detecting other electrical and mechanical faults.

7 References

[1] Metwally, Ibrahim A. "Failures, monitoring and new trends of power transformers." *IEEE potentials* 30.3 (2011): 36-43.

[2] Li, Shuaibing, et al. "Interpretation of DGA for transformer fault diagnosis with complementary SaE-ELM and arctangent transform." *IEEE Transactions on Dielectrics and Electrical Insulation* 23.1 (2016): 586-595.

[3] Bigdeli, Mehdi, Mehdi Vakilian, and Ebrahim Rahimpour. "A probabilistic neural network classifier-based method for transformer winding fault identification through its transfer function measurement." *International Transactions on Electrical Energy Systems* 23.3 (2013): 392-404.

[4] Tarimoradi, Hadi, and Gevork B. Gharehpetian. "Novel calculation method of indices to improve classification of transformer winding fault type, location, and extent." *IEEE Transactions on Industrial Informatics* 13.4 (2017): 1531-1540.

[5] Abbasi, Ali Reza, and Mohammad Reza Mahmoudi. "Application of statistical control charts to discriminate transformer winding defects." *Electric Power Systems Research* 191 (2021): 106890.

[6] Ghanizadeh, Ahmad Javid, and G. B. Gharehpetian. "ANN and cross-correlation based features for discrimination between electrical and mechanical defects and their localization in transformer winding." *IEEE Transactions on Dielectrics and Electrical Insulation* 21.5 (2014): 2374-2382.

[7] Moradzadeh, Arash, and Kazem Pourhossein. "Early detection of turn-to-turn faults in power transformer winding: An experimental study." *2019 International Aegean Conference on Electrical Machines and Power Electronics (ACEMP) & 2019 International Conference on Optimization of Electrical and Electronic Equipment (OPTIM)*. IEEE, 2019.

[8] Moradzadeh, Arash, and Kazem Pourhossein. "Application of support vector machines to locate minor short circuits in transformer windings." *2019 54th International Universities Power Engineering Conference (UPEC)*. IEEE, 2019.

[9] Moradzadeh, Arash, et al. "Turn-to-turn short circuit fault localization in transformer winding via image processing and deep learning method." *IEEE Transactions on Industrial Informatics* 18.7 (2021): 4417-4426.

[10] Nosratian Ahour, Jafar, Saeed Seyedtabaii, and Gevork B. Gharehpetian. "Determination and localisation of turn-to-turn fault in transformer winding using frequency response analysis." *IET Science, Measurement & Technology* 12.3 (2018): 291-300.

[11] Aghmasheh, Reza, Vahid Rashtchi, and Ebrahim Rahimpour. "Gray box modeling of power transformer windings based on design geometry and particle swarm optimization algorithm." *IEEE transactions on power delivery* 33.5 (2018): 2384-2393.

[12] Rahimpour, Ebrahim, et al. "Transfer function method to diagnose axial displacement and radial deformation of transformer windings." *IEEE Transactions on power delivery* 18.2 (2003): 493-505.

[13] Rahimpour, Ebrahim, Mehdi Jabbari, and Stefan Tenbohlen. "Mathematical comparison methods to assess transfer functions of transformers to detect different types of mechanical faults." *IEEE transactions on power delivery* 25.4 (2010): 2544-2555.

[14] Dua, Wenxia, et al. "The Fault Detection of Power Transformers Based on Kernel Principal Component Analysis."

[15] Schölkopf, Bernhard, Alexander Smola, and Klaus-Robert Müller. "Kernel principal component analysis." *International conference on artificial neural networks*. Berlin, Heidelberg: Springer Berlin Heidelberg, 1997.